A Photonic Terahertz Interferometric Inverse Synthetic Aperture Radar Scheme for High Resolution 3D Positioning

Zuomin Yang[1], Hongqi Zhang[1], Zhidong Lyu[1], Hang Yang[1], Lu Zhang[1], Xianbin Yu[2*]
[1]*College of Information Science and Electronic Engineering, Zhejiang University, 310027 Hangzhou, China*
[2]*Zhejiang Lab, Hangzhou 311121 China*
*E-mail: xyu@zhejianglab.com

***Abstract*—A photonic terahertz interference inverse synthetic aperture radar scheme is proposed and demonstrated, achieving 3D positioning of corner reflectors with ~0.8 cm×~0.8 cm 2D-resolution and 0.042 cm height error over a distance of 220 cm.**

Keywords—Terahertz photonics, terahertz radar, InISAR, Positioning

I. Introduction

The terahertz band (0.1-10 THz) is between the microwave and the infrared bands, with several unique features, including good penetrability, high carrier frequency, and large bandwidth [1], [2], which makes it of great interest for Tbit/s wireless communication, mm-resolution detection and so on [3]-[6]. With the merits of large operational bandwidth and excellent penetrability, THz radar has been regarded as a new solution to the dilemmas of traditional radar systems. Compared with microwave radar, THz radar can carry broadband waveforms for performing high-resolution imaging of targets and obtaining more precise target information [7]-[9]. Compared with the Lidar and infrared radar, THz radar is robust in a variety of climatic conditions, such as snowy and foggy. Therefore, the THz radar is promising for driving assistance systems, traffic surveillance, and topographic survey [10]-[13].

To date, many studies have been devoted to the development of THz radar. Among them, synthetic aperture radar (SAR)/inverse synthetic aperture radar (ISAR) systems hold the merits of simple system structure and small time-consumption. They typically acquire the two-dimensional (2D) position information of targets by relative motion between the radar and the targets [13-15]. However, the SAR/ISAR systems can only capture 2D projected features of targets as the phase information is missing for detecting height dimension. In comparison, the interferometric SAR/ISAR (InSAR/InISAR) systems can fully tackle the information of data to reconstruct three-dimensional (3D) spatial position of targets. Some electronic InISAR systems working in the THz band have been reported [16,17], while they suffer the limited bandwidth and electromagnetic interference (EMI). Alternatively, photonic systems exhibit the well-known superiority of supporting reconfigurable and broadband waveform generation. However, only a few InISAR systems based on photonics working in the X-band have been proposed [18], [19], without any THz potential related exploration.

In this work, we propose and demonstrate a THz InISAR system based on photonics for 3D positioning. An optical frequency comb (OFC) is created for photonically generating a highly pure, flexible THz radar signal, as a benefit of the constant phase relationship between two OFC comb lines. The echoes are converted to several low-frequency components (~MHz) based on simple two-stage mixing. Next, the output signals are processed with digital positioning algorithms. The experimental results indicate that our InISAR system can accurately estimate the spatial position of multiple targets.

This paper is organized as follows. In section 2, the principle of the InISAR scheme is introduced, and then we present the experimental setup of our photonic THz InISAR system in section 3. Next, the experimental results are presented and discussed in section 4. Finally, we conclude our work in section 5.

II. Principle

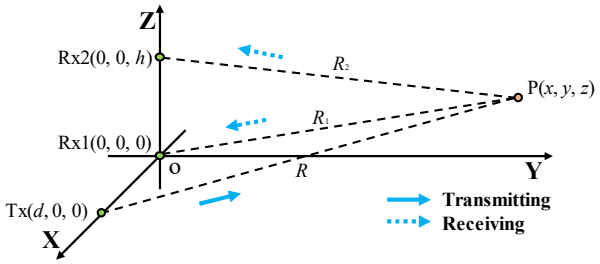

Fig. 1. The geometric schematic of InISAR with one transmitting antenna and two receiving antennas. Tx: the transmitting antenna; Rx1, Rx2: the receiving antennas; P: a representative scattering center point; R, R_1, R_2: the distances from Tx, Rx1, Rx2 to P, respectively (R, R_1, $R_2 >> h$, d).

The geometric schematic of InISAR is shown in Fig. 1, which is composed of one transmitting antenna (Tx (d, 0, 0)) and two receiving antennas (Rx1 (0, 0, 0), Rx2 (0, 0, h)) at different heights. P (x, y, z) is a representative scattering central point to illustrate the principle. R, R_1, R_2 are the distances from Tx, Rx1, Rx2 to P (R, R_1, R_2>>d, h), and we can get $R_1 \approx R_2 \approx y$. We suppose that a linear frequency-modulated wave (LFMW) is transmitted by Tx, which can be described as:

$$s(\hat{t}, t_m) = \mathrm{rect}(\frac{\hat{t}}{T_p}) \cdot \exp[j2\pi(f_c t + \frac{k\hat{t}^2}{2})], \quad (1)$$

where rect(·) is the rectangle envelope, T_p, f_c, and k are the width of LFMW pulse, the center frequency, and the slope of frequency-modulated, $\hat{t} = t - mT$ is the fast time, t is the full time, $t_m = mT, (m = 0,1,2,\ldots,M-1)$ is the slow time, M denotes the number of accumulated pulses and T the pulse repetition period. The THz signal propagates in the free space and is reflected by the scattering center P. The echoes are down-converted by Rx1 and Rx2, and mixed with the reference signal for de-chirping. Next, phase compensation and range alignment are conducted after the Fourier transform (FT) for the fast time. Then the signals are applied the FT for the slow time, they can be approximately expressed as:

$$\mathrm{E}_1(\hat{f},f_m)=A_1\cdot T_p\cdot T_a\cdot \mathrm{sinc}[T_p(\hat{f}+\frac{R+R_1}{c}k)]\cdot \mathrm{sinc}[T_a(f_m+\frac{V+V_1}{c}f_c)] \cdot\exp[-j2\pi\frac{f_c(R+R_1)}{c}], \quad (2)$$

$$\mathrm{E}_2(\hat{f},f_m)=A_2\cdot T_p\cdot T_a\cdot \mathrm{sinc}[T_p(\hat{f}+\frac{R+R_2}{c}k)]\cdot \mathrm{sinc}[T_a(f_m+\frac{V+V_2}{c}f_c)] \cdot\exp[-j2\pi\frac{f_c(R+R_2)}{c}], \quad (3)$$

where A_1 and A_2 are the attenuation coefficients of the two channels, T_a is the time of synthetic aperture, c is the velocity of light in vacuum, $\hat{f}$, f_m are the frequencies corresponding to the fast and slow time. The parameters of V, V_1 and V_2 are the relative velocities between Tx, Rx1, Rx2 and P, respectively. Supposing that the small rotation condition is satisfied and the angular velocity of the equivalent rotational model is ω, we can get $V_1=V_2=\omega x$. So far, the relationship between the frequency and the 2D-coordinates (x, y) of the P is established. Next, interfering the two complex 2D image signals, we can obtain:

$$\Delta\varphi=angle(E_1\cdot E_2^*)=\frac{2\pi}{\lambda_c}(R_2-R_1). \quad (4)$$

The relationship between the position parameters can be derived from Fig. 1:

$$x^2+y^2+z^2=R_1^2, \quad (5)$$

$$x^2+y^2+(z-h)^2=R_2^2, \quad (6)$$

Then combining the (2)-(6), the 3D coordinate of P (x, y, z) can be established:

$$x=\frac{\lambda_c}{2\omega}\cdot f_m, \quad (7)$$

$$y=\frac{c}{2k}\cdot \hat{f}, \quad (8)$$

$$z=-\frac{\Delta\varphi\cdot\lambda_c\cdot y}{2\pi h}+\frac{h}{2}. \quad (9)$$

Such, the scattering center P is well localized in 3D space. It is noted that, the interference phase $\Delta\varphi$ should be in the range of $[-\pi,\pi]$, otherwise the phase will be wrapped, i.e., the height range should satisfy

$$-\frac{\lambda_c\cdot R}{2h}+\frac{h}{2}\le z\le\frac{\lambda_c\cdot R}{2h}+\frac{h}{2}. \quad (10)$$

III. Experiment

The experimental setup of the proposed system is shown in the left of Fig. 2. The right of Fig. 2 gives the photo of the platform and link, and the actual spatial position of three antennas are displayed in the lower left. A laser (NKT) is used to emit a 16 dBm optical carrier at a frequency of 193.414 THz. A phase modulator (PM, EOSPACE) is used to create an OFC driven by a 30 dBm RF signal at a frequency of 28 GHz. The optical spectrum of the generated OFC is shown in Fig. 3(a). Next, a waveshaper (WS1, Waveshaper 4000A, Finisar) filters out two optical frequency components as a stable carrier and a local oscillator at 193.554 THz and 193.274 THz, as shown in Fig. 3(b). A broadband LFM signal from 10 GHz to 30 GHz with a pulse width of 4 us is generated by an arbitrary waveform generator (AWG, 8194A, Keysight). Here the LFM signal is split into two divisions. One is used to modulate the optical carrier at the frequency of 193.554 THz (Branch1) via a dual-parallel Mach-Zehnder modulator (DPMZM, OMFT-C-00-FA, IDPHOTONICS), and the other is regarded as a reference signal. The desirable signal after the DPMZM is selected by a waveshaper (WS2, Waveshaper 100s, Finisar) from the double sideband modulated signals, as shown in Fig. 3(c). The red frame indicates the selected signal, which is an LFM signal with a bandwidth from 193.564 THz to 193.584 THz. The selected optical components and the local oscillator are power balanced at 14.5 dBm by using two erbium doped fiber amplifiers (EDFA) and then combined, as shown in Fig. 3(d). A weak single frequency near the LFM modulation is observed due to limited rejection level of the WS1, which can be mitigated during the following de-chirping. The combined optical signals are then injected into a uni-traveling-carrier photodiode (UTC-PD, IOD-PMJ-13001, NTT) to generate and radiate a terahertz LFM wave propagating in the free space towards targets. A polarization controller (PC) and a polarizer are used to align the incoming optical waves with the UTC-PD.

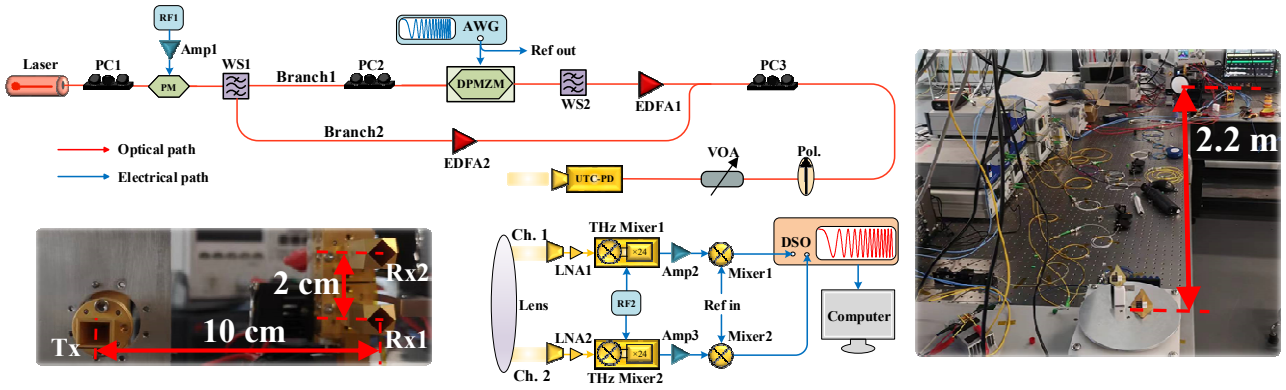

Fig. 2. The left is the experimental setup of the proposed THz InISAR system. PC: Polarization Controller. RF: Radio Frequency source. Amp: Amplifier. PM: Phase Modulator. WS: WaveShaper. EDFA: Erbium Doped Fiber Amplifier. AWG: Arbitrary Waveform Generator. DPMZM: Dual-Parallel Mach-

Zehnder Modulator. Pol: Polarizer. VOA: Variable Optical Attenuator. UTC-PD: Uni-Traveling-Carrier Photodiode. LNA: Low Noise Amplifier. DSO: Digital Storage Oscilloscope. The right is the link of the actual system and the lower left is the spatial position of the antennas.

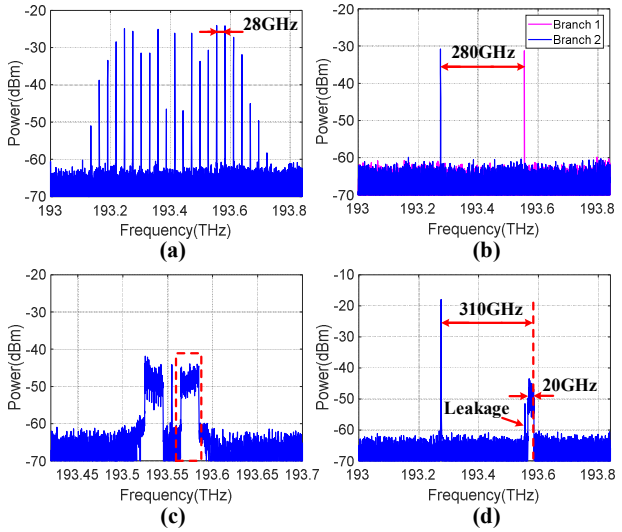

Fig. 3. Optical spectra of signals (a) after the PM, (b) after the WS1, (c) after the DPMZM and (d) after the VOA.

With respect to the reception after the reflection by targets, a lens (LMR4, THORLABS) is used to collect the THz beam. Subsequently, the terahertz signals are firstly down-converted at two THz mixers after being amplified by low noise amplifiers (LNAs) with a gain of 22 dB each (Channel 1 and Channel 2). The RF2 is at 11.584 GHz, which leads to a LO frequency at two THz-mixers of 278.013 GHz via the 24-time frequency multiplication. The echoes after THz down-conversion are amplified with a gain of 22 dB and then mixed with the reference signal from the AWG at two microwave mixers (M2-0243, Marki) for de-chirping. As a result, several single frequency components at low-frequency corresponding to different targets would be generated, captured by a digital storage oscilloscope (DSO), and processed by the InISAR algorithms. In our experiment, a turntable with controllable rotating speed is used to fulfil the conditions of InISAR, and the distance between Rx1 and the center of the turntable is 220 cm. The baseline of the two receiving antennas (h) and the distance from Tx to Rx1 (d) are 2 cm and 10 cm, respectively.

IV. Results

A photonic THz InISAR system for 3D positioning is experimentally established and conducted based on the setup in Fig. 2. Two corner reflectors (SAJ-014-S1 and SAJ-018-S1, SAGE) are fixed on the turntable and employed as targets to be imaged. The heights of the antennas and the targets are at the same level, making sure the THz beam fully illuminates the turntable and the targets. Three antennas are placed at Tx (10 cm, 0, 0), Rx1 (0, 0, 0), and Rx2 (0, 0, 2 cm), as shown in the inset of Fig. 2. In this case, the height range of accurate positioning is estimated as 11 cm from (10), and the phase-wrapped issue can be avoided.

In the experiment, the schematic diagram of reflectors placement is shown in Fig. 4(a) and (b). Their scattering centers are 3.8 cm and 5.6 cm apart in vertical and horizontal dimensions, with a height difference of 3.1 cm. The rotating speed of the turntable is set as 3.31 rad/s. The theoretical resolution of range is ~0.8 cm based on the 20 GHz bandwidth of radar signal, and the coherent accumulation angle reaches 0.0625 rad, resulting in a similar resolution of azimuth of ~0.8 cm.

The 2D positioning results of targets from two channels are shown in Fig. 4(c) and (d). From the results, we can observe that both corner reflectors are clearly positioned on the 2D plane. However, the output from Channel 1 provides a better result, this is because Rx1 and Tx sit exactly at the same height, resulting in more receiving energy from the echoes. The measured spacings of two corner reflectors are 3.74 cm in vertical direction and 5.60 cm in horizontal direction, respectively. The error of about 0.06 cm is mainly caused by the signal path difference due to the corner size-dependent internal reflection. A 3D-reconstruction of position can be obtained by interfering with these two ISAR images. Referring to coordinate origin Rx1, the spatial coordinates of two targets are (3.21 cm, 211.74 cm, 5.173 cm) and (-2.39 cm, 215.48 cm, 2.142 cm), as illustrated in Fig. 4(e). We can see that the height information is successfully reconstructed, which are close to the actual positions of targets with a maximum measurement error of about 0.042 cm.

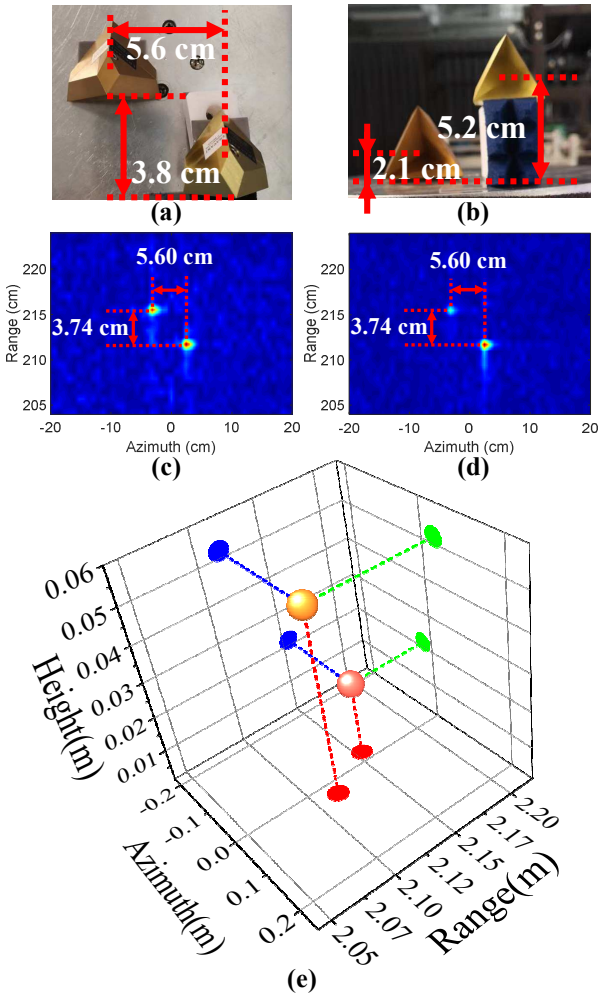

Fig. 4. The spatial position of two corner reflectors, (a) the top view and (b) the front view. (c) and (d) are the 2D positioning results of the Channel 1 and Channel 2. (e) the 3D positioning result. R: Range. A: Azimuth. H: Height.

V. Conclusion

In this paper, a THz InISAR scheme based on photonics is proposed and experimentally demonstrated, to implement

high resolution 3D positioning of multiple targets. By employing a flexible and anti-electromagnetic-interference THz photonic source, broadband THz transmitter, and fast 3D positioning InISAR algorithms, a maximum height error of 0.042 cm over a distance of 220 cm and two-dimensional resolution of ~0.8 cm×~0.8 cm have been achieved. Therefore, the proposed system has great potential in applications such as gesture recognition and express package inspection.

ACKNOWLEDGMENT

This work is supported by the National Key Research and Development Program of China (2018YFB1801500) and "Pioneer" and "Leading Goose" R&D Program of Zhejiang 2023C01139, in part by the Natural National Science Foundation of China under Grant 62101483, the Natural Science Foundation of Zhejiang Province under Grant LQ21F010015, Zhejiang Lab (no. 2020LC0AD01).

REFERENCES

[1] K. Ajito, and Y. Ueno, "THz chemical imaging for biological applications," *IEEE Trans. Terahertz Sci. Technol.*, vol. 1, no. 1, pp. 293-300, Sept. 2011.

[2] A. Ahmadivand, B. Gerislioglu, R. Ahuja, and Y. Mishra, "Terahertz plasmonics: The rise of toroidal metadevices towards immunobiosensings," *Mater. Today*, vol. 32, pp. 108-130, Jan. 2020.

[3] H. Zhang, L. Zhang, S. Wang, Z. Lu, Z. Yang, S. Liu, and X. Yu, "Tbit/s Multi-Dimensional Multiplexing THz-Over-Fiber for 6G Wireless Communication," in *J. Light. Techno.*, vol. 39, no. 18, pp. 5783-5790, Sept. 2021.

[4] S. Wang, H. Zhang, S. Jia, M. Saqlain, S. Zheng, H. Chi, X. Jin, X. Zhang, and X. Yu, "Dual-Band THz Photonic Pulses Enabling Synthetic mm-Scale Range Resolution," in *IEEE Photonics Technol. Lett.*, vol. 30, no. 20, pp. 1760-1763, Oct. 2018.

[5] H. Song and J. Song, "Terahertz-Wave Vibrometer Using a Phase-Noise-Compensated Self-Heterodyne System," in *IEEE Photonics Technol. Lett.*, vol. 28, no. 3, pp. 363-366, Feb. 2016.

[6] T. Nagatsuma, H. Nishii, and T. Ikeo, "Terahertz imaging based on optical coherence tomography," *Photonics Res.*, vol. 2, no. 4, pp. B64-B69, Aug. 2014.

[7] M. Caris, S. Stanko, A. Wahlen, R. Sommer, J. Wilcke, N. Pohl, A. Leuther, and A. Tessmann, "Very high resolution radar at 300 GHz," in *2014 11th European Radar Conference (EURAD)*, Rome, Italy, 2014, pp. 494-496.

[8] G. Serafino, F. Scotti, L. Lembo, B. Hussain, C. Porzi, A. Malacarne, S. Maresca, D. Onori, P. Ghelfi, and A. Bogoni, "Toward a New Generation of Radar Systems Based on Microwave Photonic Technologies," in *J. Light. Techno.*, vol. 37, no. 2, pp. 643-650, Jan. 2019.

[9] S. Pan and Y. Zhang, "Microwave Photonic Radars," in *J. Light. Techno.*, vol. 38, no. 19, pp. 5450-5484, Oct. 2020.

[10] J. Hasch, E. Topak, R. Schnabel, T. Zwick, R. Weigel, and C. Waldschmidt, "Millimeter-wave technology for automotive radar sensors in the 77 GHz frequency band," in *IEEE Trans. Microw. Theory Tech.*, vol. 60, no. 3, pp. 845–860, March 2012.

[11] L. Daniel, D. Phippen, E. Hoare, A. Stove, M. Cherniakov, and M. Gashinova, "Low-THz radar, lidar and optical imaging through artificially generated fog," International Conference on Radar Systems (Radar 2017), 1-4 (2017).

[12] S. Wang, Z. Lu, N. Idrees, S. Zheng, X. Jin, X. Zhang, and X. Yu, "Photonic generation and de-chirping of broadband THz linear-frequency-modulated signals, " IEEE Photonics Technol. Lett. 31(11), 881-884 (2019).

[13] L. Daniel, D. Phippen, E. Hoare, A. Stove, M. Cherniakov, and M. Gashinova, "Low-THz radar, lidar and optical imaging through artificially generated fog," in *International Conference on Radar Systems (Radar 2017)*, United Kingdom, 2017, pp. 1-4.

[14] M. Liang, C. Zhang, R. Zhao, and Y. Zhao, "Experimental 0.22 THz stepped frequency radar system for ISAR imaging," *J. Infrared Millim. Terahertz Waves*, vol. 35, pp. 780-789, June 2014.

[15] Q. Yang, Y. Qin, K. Zhang, B. Deng, X. Wang, and H. Wang, "Experimental research on vehicle-borne SAR imaging with THz radar," *Micro. Opt. Technol. Lett.*, vol. 59, no. 8, pp. 2048-2052, May 2017.

[16] Y. Zhang, Q. Yang, B. Deng, Y. Qin, and H. Wang, "Experimental Research on Interferometric Inverse Synthetic Aperture Radar Imaging with Multi-Channel Terahertz Radar System," *Sensors*, vol. 19, no. 10, pp. 2330-2345, May 2019.

[17] H. Li, C. Li, S. Wu, S. Zheng, and G. Fang, "Adaptive 3D Imaging for Moving Targets Based on a SIMO InISAR Imaging System in 0.2 THz Band," *Remote Sens.*, vol. 13, no. 4, pp. 782-802, Feb. 2021.

[18] P. Ghelfi, F. Laghezza, F. Scotti, G. Serafino, A. Capria, S. Pinna, D. Onori, C. Porzi, M. Scaffardi, A. Malacarne, V. Vercesi, E. Lazzeri, F. Berizzi, and A. Bogoni, "A fully photonics-based coherent radar system," *Nature*, vol. 507, pp. 341-345, March 2014.

[19] D. Wu, S. Li, X. Xue, X. Xiao, S. Peng, and X. Zheng, "Photonics based microwave dynamic 3D reconstruction of moving targets," *Opt. Express*, vol. 26, no. 21, pp. 27659-27667, Oct. 2018.